Rate Constant of the HONO + HONO → H_2O + NO + NO_2 Reaction from ab Initio MO and TST Calculations

A. M. Mebel[†] **and M. C. Lin***

Department of Chemistry, Emory University, Atlanta, Georgia 30322

C. F. Melius

Combustion Research Facility, Sandia National Laboratories, Livermore, California 94552

Received: October 24, 1997; In Final Form: January 8, 1998

Kinetics and mechanism for the bimolecular decomposition of HONO have been studied by ab initio molecular orbital (G2M) and transition-state theory calculations. The reaction can take place by the interaction of a cis and a trans isomer or two cis or two trans isomers, via four-, five-, and six-member ring transition states, with decreasing reaction barriers as the size of the ring increases. The lowest energy path with a 13.7 kcal/mol barrier was found to occur by the six-member ring **TS1** formed by the reaction of *cis*- and *trans*-HONO. A similar six-member ring TS (**TS2**) formed by two cis isomers has a barrier height of 15.1 kcal/mol, which is very close to the 5-ring TS formed by two trans isomers, 15.7 kcal/mol. The total rate constant computed with the ab initio MO results, including the three reaction channels mentioned above and an additional channel involving a five-member ring TS formed by a cis- and a trans isomer with a 17.7 kcal/mol barrier, can be represented by the three-parameter expression for the 300−5000 K temperature range: $k = 5.8 \times 10^{-25} T^{3.64} \exp(-6109/T)$ cm^3/(molecule·s), which includes the Boltzmann-averaged contribution of the cis isomer. The theoretical value was found to be considerably lower than the available experimental results (which are believed to have suffered from deleterious surface effects).

I. Introduction

Nitrous acid (HONO) is a key reactive intermediate in the combustion of many nitramine propellants.[1−4] It also plays an important role in the chemistry of the polluted troposphere,[5] in which HONO may be formed by the decomposition of organic nitrates and by the exothermic termolecular reaction, NO + NO_2 + H_2O → 2HONO, possibly initiated by lightning, for example.

Over the years, the bimolecular decomposition of HONO has received much attention[6−11] because of its relevance to the chemistries of practical significance as alluded to above. The higher stability of HONO in comparison with that of HNO may result in the accumulation of HONO during the course of chemical reactions in the H/N/O systems,[12] particularly at low temperatures. The direct oxidation of HNO by NO_2, which produces HONO and NO, has been shown to occur with a barrier of 5−6 kcal/mol according to the results of our high-level ab initio MO calculations.[13] The accumulation of HONO at low temperatures, at which the rate of its unimolecular decomposition is slow, renders the bimolecular decomposition process competitive.

There have been several experimental studies in conjunction with the kinetics of the bimolecular decomposition process producing NO, NO_2, and H_2O.[6−11] The results of these studies, carried out primarily at ambient temperature for either the forward[8−11] or the reverse[6,7] reaction, vary widely, strongly suggesting the involvement of a heterogeneous process.[7,11] The rate constant for the forward reaction reported by Chan et al.,[10] $k = 1 \times 10^{-18}$ cm^3/(molecule·s) at 296 K, with the direct detection of HONO by FTIR spectrometry is higher by 2 orders of magnitude than the upper limit set by Kaiser and Wu,[11] $k \leq 1 \times 10^{-20}$ cm^3/(molecule·s) at 300 K by mass spectrometry.

Most of these results, including those reported for the reverse process (which are equally scattered) will be compared with our theoretically predicted values. The methods of our calculations, including that employed for rate constant evaluation, are described below.

II. Calculation Methods

The geometries of the reactants, products, intermediates, and transition states have been optimized using the hybrid density functional B3LYP method[14] with the 6-311G(d,p) basis set.[15] Vibrational frequencies, calculated at the B3LYP/6-311G(d,p) level, have been used for the characterization of stationary points, zero-point energy (ZPE) correction, and transition-state theory (TST) computations of the reaction rate constants. Calculated transition states have been confirmed to have one imaginary frequency. All the energies quoted and discussed in the present paper include the ZPE correction.

To obtain more reliable energies, we carried out QCISD(T)/6-311G(d,p),[16] restricted closed-shell and open-shell coupled cluster RCCSD(T)/6-311G(d,p),[17] as well as G2M(RCC,MP2)[18] calculations. The G2M(RCC,MP2) method is a modification of the Gaussian-2 (G2) approach;[19] it uses B3LYP/6-311G(d,p) optimized geometries and ZPE corrections and substitutes the QCISD(T)/6-311G(d,p) calculation of the original G2 scheme by the RCCSD(T)/6-311G(d,p) calculation. The total energy in G2M(RCC,MP2) is calculated as follows:[18]

[†] Present address: Institute of Atomic and Molecular Sciences, Academia Sinica, P.O. Box 23-166, Taipei, Taiwan.

S1089-5639(97)03449-X CCC: $15.00
Published on Web 02/12/1998

TABLE 1: Calculated Relative Energies of Transition States for the HONO + HONO Reactions

	ZPE[a]	B3LYP/ 6-311G(d,p)	MP2/ 6-311G(d,p)	CCSD(T)/ 6-311G(d,p)	QCISD(T)/ 6-311G(d,p)	MP2/ 6-311+G(3df,2p)	G2M(RCC,MP2)	BAC-MP4
trans-HONO[b]	12.7	−205.761 78	−205.274 58	−205.301 43	−205.303 35	−205.403 52	−205.508 01	
cis-HONO[b]	12.7	−205.762 15	−205.274 93	−205.301 97	−205.303 63	−205.402 80	−205.507 51	
		−0.2[c]	−0.2[c]	−0.3[c]	−0.2[c]	+0.5[c]	+0.3 (+0.5)[c,d]	−1.4[c]
TS1[e]	23.8	6.9	8.2	13.9	13.9	8.1	13.7	12.2
TS2[f]	23.8	8.4	10.4	16.1	15.8	9.4	15.1	14.8
TS3[g]	24.3	6.8	8.5	15.6	15.4	8.6	15.7	
TS4[e]	24.2	8.4	10.4	18.1	18.1	10.0	17.7	18.1
TS5[f]	23.1	19.7	18.8	26.1	26.0	18.7	26.0	
$ONNO_2 + H_2O$[g]	23.8	4.6	−7.8	0.3		−9.6	−1.5	−0.9
$ONONO + H_2O$[g]	22.7	5.8	2.4	4.7		0.8	3.2	4.1
$H_2O+NO+NO_2$[g]	21.7	6.8	3.0	5.2		5.3	10.7 [7.5][h] (7.7)[d]	4.6

[a] Zero-point energy corrections (kcal/mol), calculated at the B3LYP/6-311G(d,p) level. [b] Total energies for HONO are given in hartrees. The BAC-MP4 calculated heats of formation at 0 K are −16.1 kcal/mol for *trans*-HONO and −17.5 kcal/mol for *cis*-HONO vs −17.4 and −16.9 kcal/mol, respectively, in experiment.[24] [c] Relative energy with respect to *trans*-HONO. [d] In parentheses: experimental value taken from JANAF Thermochemical Tables.[24] [e] Relative energies with respect to *trans*-HONO + *cis*-HONO. [f] Relative energies with respect to *cis*-HONO + *cis*-HONO. [g] Relative energies with respect to *trans*-HONO + *trans*-HONO. [h] The value in brackets is computed without HLC correction.

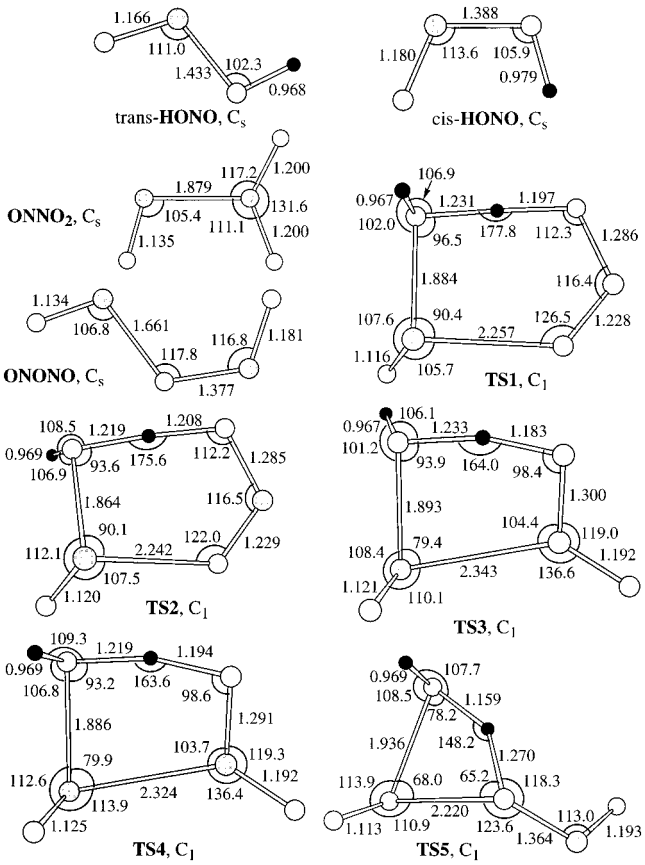

Figure 1. B3LYP/6-311G(d,p) optimized geometries of the reactants, intermediates, and transition states of the HONO + HONO reaction.

$$E[\text{G2M(RCC,MP2)}] = E[\text{RCCSD(T)/6-311G(d,p)}] + \Delta E(+3\text{df,2p}) + \Delta E(\text{HLC}) + \text{ZPE}$$

where

$$\Delta E(+3\text{df2p}) = E[\text{MP2/6-311+G(3df,2p)}] - E[\text{MP2/6-311G(d,p)}]$$

and the empirical "higher level correction" in mhartree

$$\Delta E(\text{HLC}) = -5.25n_\beta - 0.19n_\alpha$$

where n_α and n_β are the numbers of α and β valence electrons, respectively.

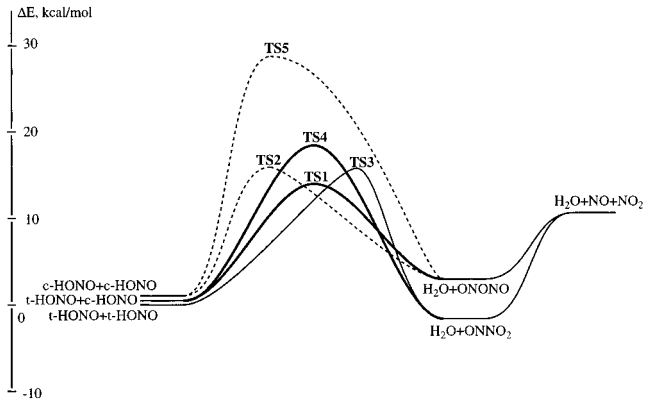

Figure 2. Profile of the potential energy surface for the HONO + HONO → H_2O + NO + NO_2 reaction, calculated at the G2M(RCC,MP2) level.

The results of these calculations are compared with those obtained by the bond-additivity corrected fourth-order Møller−Plesset perturbation theory (BAC-MP4) technique.[20] The BAC-MP4 method is known to give reliable data for many H/N/O systems.[12,21]

GAUSSIAN 94[22] and MOLPRO 96[23] programs were employed for the potential energy surface computations. Optimized geometries of various species are shown in Figure 1, and their energies are presented in Table 1. Potential energy surface of the reaction is illustrated in Figure 2.

III. Results and Discussion

A. Ab Initio MO Calculations of the Potential Energy Surface. The reaction of two HONO molecules can proceed by a hydrogen transfer from one HONO to the O(H) atom of the second molecule accompanied by elimination of H_2O. The reaction products are H_2O + NO + NO_2. The reaction is endothermic by 7.7 kcal/mol according to the experimental heats of formation $\Delta H°_f$ (0 K) taken from the JANAF Tables.[24] At the G2M(RCC,MP2) level, the calculated heat of the reaction is 10.7 kcal/mol. However, if the empirical HLC correction is not included, the theoretical reaction endothermicity is 7.5 kcal/mol, close to the experimental value. The HLC correction is due to the change of the number of electron pairs in the products as compared to that in the reactants; two radicals, NO and NO_2, are formed. On the other hand, the number of electron pairs does not formally change in transition states for the reaction, and the HLC correction cancels out. Therefore, we expect the

calculated barrier heights to have an accuracy of 1−2 kcal/mol, characteristic for the G2M method.[18]

The HONO + HONO reaction can have intermediates of the N_2O_3 stoichiometry. We considered two isomers of N_2O_3, $ONNO_2$, and ONONO. As seen in Figure 1, the structure of $ONNO_2$ is characterized by a very long NN bond, 1.88 Å. The geometries of the NO and NO_2 fragments are close to those of free NO and NO_2 radicals, respectively. The energy of formation of $ONNO_2$ from NO and NO_2 is calculated to be low, 12.2 kcal/mol at the G2M(RCC,MP2) level. If the HLC correction is excluded, the binding energy between the two radicals decreases to 9.0 kcal/mol. At room temperature, Gibbs free energies of $ONNO_2$ and NO + NO_2 are close to each other. At higher temperatures, the Gibbs free energy of two radicals is lower than that of $ONNO_2$, indicating that the complex is unlikely to exist under combustion conditions. The second isomer of N_2O_3, ONONO, is a NO-substituted analogue of HONO and might exist in four conformations, trans−cis, trans−trans, cis−trans, and cis−cis. As an example, we calculated here only a trans−cis structure. The ON−ONO bond is found to be long, 1.66 Å, but significantly shorter than the NN bond in $ONNO_2$. The geometry of the ONO fragment is close to that of *cis*-HONO, while the NO bond length in the ON fragment is about 0.01 Å shorter than the bond in the free NO radical. ONONO lies higher in energy than $ONNO_2$. The calculated binding energy with respect to NO + NO_2 is 7.5 and 4.3 kcal/mol at the G2M level with and without HLC correction, respectively, because of the low binding energy ONONO would not be stable even at ambient temperature and should dissociate producing the NO and NO_2 radicals. The initial step of the HONO + HONO reaction leading to H_2O + N_2O_3 is nearly thermoneutral, 1.5 kcal/mol exothermic for the $ONNO_2$ product and 3.2 kcal/mol endothermic for ONONO.

The transition states for the HONO + HONO → H_2O + NO + NO_2 reaction can have a six-member, five-member, or four-member ring geometry. First, we consider the six-member ring structures. The six-member cycle is formed by all four atoms of the attacking *cis*-HONO molecule (the one that donates its hydrogen atom) and by the N and O(H) atoms of the second HONO. The attacked (accepting the hydrogen atom) HONO can be either in trans or in cis conformation. The respective transition states are **TS1** (for the *cis*-HONO + *trans*-HONO reaction) and **TS2** (for the *cis*-HONO self-reaction). The energy of **TS1** is somewhat lower than that of **TS2**. The barriers relative to the reactants are calculated to be 13.7 and 15.1 kcal/mol for **TS1** and **TS2**, respectively, at our best G2M(RCC,-MP2) level. Note that the B3LYP and MP2 approximations significantly underestimate the barrier (by 5−7 kcal/mol; see Table 1). At the CCSD(T) and QCISD(T) levels with the 6-311G(d,p) basis set, the results are close to the G2M values, and the ΔE(+3df,2p) correction computed at the MP2 level is small, less than 1 kcal/mol. Since the QCISD(T) and CCSD-(T) energies are similar here, the G2M result should be close to the result of the original G2 method.

The geometries of **TS1** and **TS2** look alike, except the conformation of the attacked HONO molecule. The forming and breaking OH bonds are nearly equal, 1.20−1.23 Å. The N−O(H) bond in the attacking molecule is shortened from 1.39 Å in *cis*-HONO to 1.29 Å in the transition states. On the other hand, the N−O(H) distance in the attacked HONO is elongated by ∼0.5 Å to 1.86−1.88 Å. The bond is cleaved in the HONO + HONO → H_2O + NO + NO_2 reaction. The changes in the other two NO bond lengths are less significant. The distance between the nitrogen atom of the attacked HONO and the terminal oxygen of the attacking molecule is long, 2.24−2.26 Å. The intrinsic reaction coordinate (IRC) calculations[25] in the direction of products indicate the formation of a new NO bond and result in *trans,cis*-ONONO + H_2O. At the next step, ONONO dissociates to NO + NO_2.

Transition states **TS3** and **TS4** have five-member ring geometries. The cycle is formed by the HON fragment of the attacking *trans*-HONO in addition to the N and O(H) atoms of the second molecule. The interatomic distances in **TS3** and **TS4** are close to the distances in **TS1** and **TS2**. The breaking OH bond length in **TS3** and **TS4** is ∼0.01 Å shorter while the breaking NO bond length is 0.01−0.02 Å longer than those in **TS1** and **TS2**. The terminal NO bond of the attacking *trans*-HONO which does not participate in the cycle formation is elongated by 0.03 Å as compared to that in the reactant. In **TS1** and **TS2**, where this bond takes part in the ring, it is stretched by 0.05 Å to 1.23 Å. The NN distance in the cycle is 2.32−2.34 Å. The IRC calculations confirm that the NN bond is formed after the transition states are cleared, and the immediate products are H_2O + $ONNO_2$. The $ONNO_2$ complex then dissociates producing the NO and NO_2 radicals. The HON angle in the donor HONO molecule of **TS3** and **TS4** is 98−99° compared to 112° in **TS1** and **TS2** and 102−106° in free HONO. The OHO fragment with the angle of 164° deviates from the linearity in **TS3** and **TS4** to a higher extent than that in **TS1** and **TS2** (176−178°). The energies of **TS3** and **TS4** are higher than those of **TS1** and **TS2**. The calculated barrier for the *trans*-HONO self-reaction via **TS3** is 15.7 kcal/mol and the barrier for the *cis*-HONO + *trans*-HONO reaction via **TS4** is 17.7 kcal/mol, 4 kcal/mol higher than the barrier at **TS1**.

TS5 is an example of the four-member ring transition state. The cycle is formed by the OH fragment of the attacking HONO and the NO(H) fragment of the second molecule. In **TS5**, the breaking OH bond, 1.27 Å, is much longer than the forming OH bond, 1.16 Å. The OHO fragment is far from linear with the angle of 148°. The breaking NO bond in the attacked molecule, 1.94 Å, is 0.04−0.07 Å longer than the corresponding distances in **TS1**−**TS4**. The nonbonding NO distance in the four-member ring, 2.22 Å, is similar to those in **TS1** and **TS2**. The energy of **TS5** is much higher than the energies of other transition states. The calculated barrier for the *cis*-HONO self-reaction via **TS5** is 26.0 kcal/mol at the G2M level, more than 10 kcal/mol higher than the barrier at **TS2**. Therefore, we do not expect that the reaction channel through the four-member ring transition state can compete with the channels proceeding via **TS1**-**TS4**. While **TS5** is a transition state for the cis + cis reaction, one can imagine a total of four transition states of the four-member ring type. Besides **TS5**, these can include transition states for the cis + trans, trans + cis, and trans + trans reactions. However, since the energy of the four-member ring **TS5** is high, we did not look for the other transition states of this type.

As seen in Table 1, the agreement between the G2M and BAC-MP4 relative energies of transition states and intermediates ($ONNO_2$ + H_2O and ONONO + H_2O) is within 1−2 kcal/mol. For the overall HONO + HONO → H_2O + NO + NO_2 reaction endothermicity, the BAC-MP4 method underestimates the experimental value by ∼3 kcal/mol.

B. TST Calculations of the Rate Constants. Hereafter, we consider that the HONO + HONO → H_2O + NO + NO_2 reactions go through **TS1**−**TS4** and calculate the rate constants employing the transition-state theory.[26,27] For the calculations, we use the G2M(RCC,MP2) barrier heights and the B3LYP/

TABLE 2: Molecular and Transition-State Parameters of the Reactants and Transition States of the HONO + HONO Reactions, Used for the TST Calculations of the Rate Constants (Calculated at the B3LYP/6-311G(d,p) Level)

species	*i*	I_i (10^{-40} g cm^2)	ν_j (cm^{-1})
trans-HONO	A	8.987	589, 623, 837, 1296, 1787, 3771
	B	67.36	
	C	76.34	
cis-HONO	A	10.07	665, 722, 945, 1338, 1639, 3656
	B	63.24	
	C	73.36	
TS1	A	146.9	1002*i*, 52, 186, 234, 262, 370, 422,
	B	325.0	544, 595, 647, 810, 866, 1272,
	C	442.0	1440, 1491, 1638, 2027, 3791
TS2	A	139.3	1031*i*, 64, 200, 215, 260, 353, 435,
	B	331.0	577, 586, 639, 819, 880, 1275,
	C	452.2	1435, 1537, 1600, 1998, 3766
TS3	A	155.9	940*i*, 88, 155, 235, 287, 377, 453,
	B	340.2	559, 573, 631, 834, 880, 1255,
	C	471.6	1480, 1610, 1768, 1995, 3780
TS4	A	156.1	974*i*, 89, 158, 235, 281, 351, 464,
	B	340.6	561, 575, 623, 848, 875, 1260,
	C	478.8	1486, 1609, 1756, 1970, 3766

6-311G(d,p) molecular parameters of the reactants and transition states presented in Table 2. We use the conventional TST method with Wigner's tunneling correction described earlier.[27] The Arrhenius plots of various rate constants for the HONO + HONO reactions are shown in Figure 3, and the rate constant expressions which resulted from three- and two-parameter fitting are presented in Table 3.

The lowest barrier is calculated for the reaction

$$\textit{cis}\text{-HONO} + \textit{trans}\text{-HONO} \rightarrow \mathbf{TS1} \rightarrow H_2O + NO + NO_2 \quad (1)$$

and the rate constant k_1 is the highest among the four considered channels. For the 300−1000 K temperature range, two-parameter fitting gives an A factor of 1.4×10^{-13} cm^3/(molecule·s) and the apparent activation energy is 15.2 kcal/mol. The same reaction going via **TS4**

$$\textit{cis}\text{-HONO} + \textit{trans}\text{-HONO} \rightarrow \mathbf{TS4} \rightarrow H_2O + NO + NO_2 \quad (4)$$

is slower because the barrier is 4 kcal/mol higher. The A factor and the apparent activation energy for k_4 are 9.0×10^{-14} cm^3/(molecule·s) and 19.1 kcal/mol, respectively. The total rate constant for the cis + trans reaction, $k_1 + k_4$, is close to k_1 at the temperatures below 1000 K. At higher temperatures, the contribution of k_4 increases up to 40% of k_1.

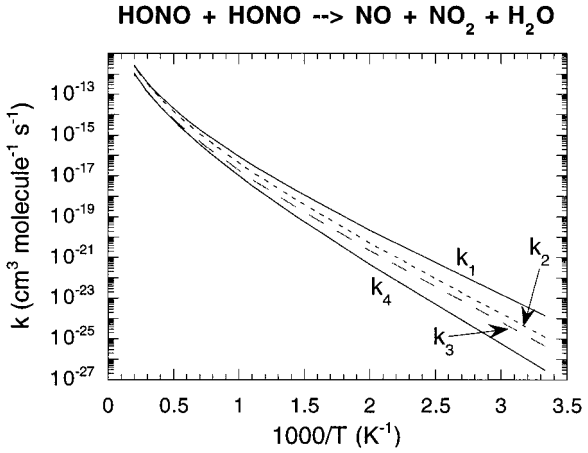

Figure 3. Arrhenius plots of the calculated rate constants for various channels of the HONO + HONO reaction.

The cis + cis reaction with transition state **TS2**:

$$\textit{cis}\text{-HONO} + \textit{cis}\text{-HONO} \rightarrow \mathbf{TS2} \rightarrow H_2O + NO + NO_2 \quad (2)$$

is also slow and k_2 can be effectively given by $k_2 = 1.45 \times 10^{-13} \exp(-16696/RT)$ cm^3/(molecule·s) for 300 K ≤ T ≤ 1000 K. The slowest reaction involves two *trans*-isomers of HONO and proceeds via **TS3**:

$$\textit{trans}\text{-HONO} + \textit{trans}\text{-HONO} \rightarrow \mathbf{TS3} \rightarrow H_2O + NO + NO_2 \quad (3)$$

At ambient temperatures, k_3 has an A factor of 6.7×10^{-14} cm^3/(molecule·s) and an apparent activation energy of 16.8 kcal/mol.

The calculated rate constants for the four lower energy paths are summarized in Table 3. To compare with the data available in the literature, which were mostly determined at ambient temperatures between 296 and 300 K for both forward and reverse directions, without differentiating the geometric isomers, we have calculated the total rate constants at 300 K by taking into account the Boltzmann-averaged concentration of the cis isomer in reactions 1, 2, and 4, $k = \sum k_i (i = 1-4) = 9.2 \times 10^{-25}$ cm^3/(molecule·s). As is evident from the results presented in the table, all existing data except the upper limit set by Kaiser and Wu,[11] $k < 1 \times 10^{-20}$ cm^3/(molecule·s) at 300 K, are higher than the predicted value by several orders of magnitude. Kaiser and Wu attributed the high values of most reported results and the large discrepancy among them to heterogeneous surface effects, which are usually not insignificant for such highly polar

TABLE 3: Fitted Expressions for the Rate Constants of the HONO + HONO Reactions (in Units of cm^3/(molecule·s))

reaction	300 K ≤ T ≤ 5000 K	300 K	300 K ≤ T ≤ 1000 K
cis + trans, k_1	$1.41 \times 10^{-24} T^{3.46} \exp(-5920/T)$	1.4×10^{-24}	$1.40 \times 10^{-13} \exp(-7650/T)$
cis + trans, k_4	$1.41 \times 10^{-24} T^{3.40} \exp(-7926/T)$	1.2×10^{-27}	$9.04 \times 10^{-14} \exp(-9630/T)$
cis + trans, $k_1 + k_4$	$3.96 \times 10^{-25} T^{3.65} \exp(-5866/T)$		$1.54 \times 10^{-13} \exp(-7684/T)$
cis + cis, k_2	$1.23 \times 10^{-24} T^{3.48} \exp(-6664/T)$	1.2×10^{-25}	$1.45 \times 10^{-13} \exp(-8403/T)$
trans + trans, k_3	$1.32 \times 10^{-24} T^{3.36} \exp(-6764/T)$	4.5×10^{-26}	$6.67 \times 10^{-14} \exp(-8456/T)$
theory	$\sum k_i$ at 300 K	9.2×10^{-25}	
experiment[a]	Wayne and Yost[b]	3×10^{-15}	
	Graham and Tyler[c]	8×10^{-19}	
	Cox and Derwent[d]	2×10^{-21}	
	England and Corcoran[e]	9×10^{-18}	
	Chan et al.[f]	1×10^{-18}	
	Kaiser and Wu[g]	$<1 \times 10^{-20}$	

[a] The reverse rate constant was converted to the forward value with the equilibrium constant, $K = 7.0 \times 10^2$ Torr at 300 K.[11] [b] Reference 6. [c] Reference 7. [d] Reference 8. [e] Reference 9. [f] Reference 10. [g] Reference 11.

and labile reactants as HONO. In a temperature-dependent study, carried out by kinetic modeling for the oxidation of NO at ppm levels in wet air, England and Corcoran[9] obtained an Arrhenius expression for the HONO + HONO reaction, $k = 1.7 \times 10^{-11} \exp(-8540/RT)$ cm^3/(molecule·s), which differs greatly from our predicted equation given in Table 3. Their room-temperature result is 6 orders of magnitude higher than ours at 300 K (see Table 3).

IV. Conclusion

The bimolecular decomposition of HONO involving cis and/or trans isomers can take place by four-, five-, or six-member ring transition states with decreasing activation energies. The lowest energy path occurs by a six-member ring TS formed by *cis*- and *trans*-HONO isomers and was calculated to have a reaction barrier of 13.7 kcal/mol above the reactants.

Transition-state calculations were carried out with the computed energetics and molecular parameters. The predicted rate constant for the total disappearance of HONO was found to be considerably smaller than those reported for either the forward or the reverse process. The smaller theoretical value is, however, consistent with the upper limit set at 300 K by Kaiser and Wu,[11] who concluded that the high values of the rate constant, together with the large scatter of the existing data in the literature resulted from a heterogeneous (surface) reaction. A similar suggestion on the effect of the reactor surface was made earlier by Graham and Tyler.[7]

For the kinetic modeling of the gas-phase chemistry of the H/N/O system, our theoretical value for the total rate constant, corrected for the equilibrium concentration of the cis isomer, $k = 5.80 \times 10^{-25} T^{3.64} \exp(-6109/T)$ cm^3/(molecule·s), is recommended.

Acknowledgment. The authors gratefully acknowledge the support of this work by the Office of Naval Research (Contract N00014-89-J-1949) under the direction of Dr. R. S. Miller. We thank the Cherry L. Emerson Center for Scientific Computation for the use of computing facilities and various programs.

References and Notes

(1) Kuo, K. K.; Summerfield, M. *Fundamentals of Solid Propellant Combustion, Progress in Astronautics and Aeronautics*; AIAA, Inc.: New York, 1984; Vol. 90.

(2) Alexander, M. H.; Dagdigian, P. J.; Jacox, M. E.; Kolb, C. E.; Melius, C. F.; et al. *Prog. Energy Combust. Sci.* **1991**, *17*, 263.

(3) Adams, G. F.; Shaw, R. W., Jr. *Annu. Rev. Phys. Chem*. **1992**, *43*, 311.

(4) Mebel, A. M.; Lin, M. C.; Morokuma, K.; Melius, C. F. *J. Phys. Chem.* **1995**, *99*, 6842.

(5) Atkinson, R. J. *Phys. Chem. Ref. Data*, Monograph 2, Gas-Phase Tropospheric Chemistry of Organic Compounds, 1993.

(6) Wayne, L. G.; Yost, D. M. *J. Chem. Phys.* **1951**, *19*, 41.

(7) Graham, R. F.; Tyler, B. J. *J. Chem. Soc., Faraday Trans.* 1 **1972**, *68*, 683.

(8) Cox, R. A.; Derwent, R. G. *J. Photochem*. **1976/77**, *6*, 23.

(9) England, C.; Corcoran, W. H. *Ind. Eng. Chem. Fundam.* **1975**, *14*, 55.

(10) Chan, W. H.; Nordstrom, R. J.; Calvert, J. G., Shaw, J. H. *Chem. Phys. Lett.* **1976**, *37*, 411.

(11) Kaiser, E. W.; Wu, C. H. *J. Phys. Chem.* **1977**, *81*, 1701.

(12) Diau, E. W. G.; Lin, M. C.; He, Y.; Melius, C. F. *Prog Energy Combust. Sci*. **1995**, *21*, 1.

(13) Mebel, A. M.; Lin, M. C.; Morokuma, K. *Int. J. Chem. Kinet.*, submitted.

(14) (a) Becke, A. D. *J. Chem. Phys.* **1993**, *98*, 5648; (b) *Ibid.* **1992**, *96*, 2155; (c) *Ibid.* **1992**, *97*, 9173. (d) Lee, C.; Yang, W.; Parr, R. G. *Phys. Rev. B* **1988**, *37*, 785.

(15) For the description of basis sets of the 6-311G(d,p) type see: Hehre, W. J.; Radom, L.; Schleyer, P. v. R.; Pople, J. *Ab Initio Molecular Orbital Theory*; Wiley: New York, 1986.

(16) Pople, J. A.; Head-Gordon, M.; Raghavachari, K. *J. Chem. Phys.* **1987**, *87*, 5768.

(17) (a) Purvis, G. D.; Bartlett, R. J. *J. Chem. Phys.* **1982**, *76*, 1910. (b) Hampel, C.; Peterson, K. A.; Werner, H.-J. *Chem. Phys. Lett.* **1992**, *190*, 1. (c) Knowles, P. J.; Hampel, C.; Werner, H.-J. *J. Chem. Phys.* **1994**, *99*, 5219. (d) Deegan, M. J. O.; Knowles, P. J. *Chem. Phys. Lett.* **1994**, *227*, 321.

(18) Mebel, A. M.; Morokuma, K.; Lin, M. C. *J. Chem. Phys.* **1995**, *103*, 7414.

(19) Curtiss, L. A.; Raghavachari, K.; Trucks, G. W.; Pople, J. A. *J. Chem. Phys.* **1991**, *94*, 7221.

(20) Melius, C. F., Binkley, J. S. *20th Symp. (Int.) Combust., [Proc.]* **1984**, 575.

(21) (a) Mebel, A. M., Morokuma, K.; Lin, M. C.; Melius, C. F. *J. Phys. Chem.* **1995**, *99*, 1900. (b) Hsu, C.-C.; Lin, M. C.; Mebel, A. M.; Melius, C. F. *J. Phys. Chem. A* **1997**, *101*, 60.

(22) Frisch, M. J.; Trucks, G. W.; Schlegel, H. B.; Gill, P. M. W.; Johnson, B. G.; Robb, M. A.; Cheeseman, J. R.; Keith, T.; Petersson, G. A.; Montgomery, J. A.; Raghavachari, K.; Al-Laham, M. A.; Zakrzewski, V. G.; Ortiz, J. V.; Foresman, J. B.; Cioslowski, J.; Stefanov, B. B.; Nanayakkara, A.; Challacombe, M.; Peng, C. Y.; Ayala, P. Y.; Chen, W.; Wong, M. W.; Andres, J. L.; Replogle, E. S.; Gomperts, R.; Martin, R. L.; Fox, D. J.; Binkley, J. S.; Defrees, D. J.; Baker, J.; Stewart, J. P.; Head-Gordon, M.; Gonzalez, C.; Pople, J. A. GAUSSIAN 94, Revision B.2; Gaussian, Inc.; Pittsburgh, PA, 1995.

(23) MOLPRO is a package of ab initio programs written by H.-J. Werner and P. J. Knowles, with contributions from J. Almlöf, R. D. Amos, M. J. O. Deegan, S. T. Elbert, C. Hampel, W. Meyer, K. Peterson, R. Pitzer, A. J. Stone, P. R. Taylor, and R. Lindh.

(24) Chase, M. W., Jr.; Davles, C. A.; Downey, J. R., Jr.; Frurip, D. J.; McDonald, R. A.; Syverud, A. N. JANAF Thermochemical Tables; *J. Phys. Chem. Ref. Data* **1985,** *14,* Suppl. 1.

(25) Gonzalez, C.; Schlegel, B. H. *J. Chem. Phys.* **1989**, *90*, 2154.

(26) Laidler, K. J. *Chemical Kinetics*, 3rd ed.; Harper and Row: New York, 1987.

(27) Steinfeld, J. I.; Francisco, J. S.; Hase, W. L. *Chemical Kinetics and Dynamics*; Prentice Hall: Englewood Cliffs, NJ, 1989.